

University of Richmond

UR Scholarship Repository

Honors Theses

Student Research

5-2023

Investigation of the VirA Linker Domain to Characterize its Phenol Interactions

Jessica Garofalo

Follow this and additional works at: <https://scholarship.richmond.edu/honors-theses>



Part of the [Biology Commons](#)

Recommended Citation

Garofalo, Jessica, "Investigation of the VirA Linker Domain to Characterize its Phenol Interactions" (2023). *Honors Theses*. 1726.

<https://scholarship.richmond.edu/honors-theses/1726>

This Thesis is brought to you for free and open access by the Student Research at UR Scholarship Repository. It has been accepted for inclusion in Honors Theses by an authorized administrator of UR Scholarship Repository. For more information, please contact scholarshipprepository@richmond.edu.

Investigation of the VirA Linker Domain to Characterize its Phenol Interactions

by

Jessica Garofalo

Honors Thesis

Submitted to:

Biology Department
University of Richmond
Richmond, VA

December 7, 2022

Advisor: Dr. B Daniel Pierce



(advisor signature)

12/7/22

(date)



(reader signature)

12/02/2022

(date)

Abstract

The soil bacterium *Agrobacterium tumefaciens* causes tumors in plants through interkingdom gene transfer. This transfer is initiated upon a wounding event that results in the release of plant signaling factors such as phenols and sugars that are recognized by protein machinery in the periplasm and inner membrane of *A. tumefaciens*. The histidine kinase protein VirA, in combination with the periplasmic protein ChvE, recognizes these signals and initiates induction of virulence genes via a signaling pathway, culminating with the insertion of tumor-inducing T-DNA into the wounded plant cells. While the interaction between the Periplasmic domain of VirA and sugar-bound ChvE is well-characterized, less is understood about the VirA Linker domain, which is critical for phenol reception. Indeed, experiments using VirA truncations have found that the Linker domain is essential in the recognition process of phenols through a putative direct binding. We have begun to investigate novel VirA mutations and the effect they have on signal recognition through β -galactosidase assays. Through the production and isolation of the VirA Linker domain, we aim to further characterize this region through identifying its secondary structure using circular dichroism. In addition, models have predicted that the Linker region is homologous to GAF domains, which are known to bind small ligands. Here, we currently have developed a model that predicts where phenols may bind in this region but solving the structure of the Linker domain will be necessary to fully test these predictions. In addition, we aim to directly test the interactions between the Linker domain and phenols by using fluorescence-based thermal shift assays. These assays will monitor protein folding and stability in the presence and absence of phenols at varying temperatures. Together, these data contribute to a further understanding of how phenol interaction with VirA results in autophosphorylation and signal propagation.

Introduction

Agrobacterium tumefaciens is a type of soil bacteria that causes crown gall disease in plants, resulting in tumor growth causing millions of dollars in damages annually (McCullen & Binns, 2006). *A. tumefaciens* has evolved to recognize signals, specifically sugars and phenols, that are released from plants after a wounding event, likely an indication of decreased defense mechanisms in the host plant (McCullen & Binns, 2006). Pathogenesis continues through the attachment of *A. tumefaciens* to the plant cells, creating an opening in the plant cell wall through a Type IV secretion system, followed by the insertion of a section of Transfer-DNA (T-DNA) into the plant cell to then be integrated and expressed. This T-DNA comes from a tumor inducing (Ti) plasmid that contains the genes that encode proteins that are necessary for successful tumorigenesis. The expression of this T-DNA by the plant cell leads to the production of amino acid-sugar conjugates, opines, which serves as a source of nutrients for *A. tumefaciens*.

The initial steps of pathogenesis are mediated by the histidine kinase protein VirA. VirA exists in the transmembrane region of the inner membrane of *A. tumefaciens* and functions to initiate the pathogenic response. The structure of VirA has never been experimentally solved, but models have been generated that provide insight into its structure and function. It is believed to function as a dimer and has been characterized as containing four domains: Periplasmic (P), Kinase (K), Linker (L), and Receiver (R) (Fig. 1A, B). The Linker domain has been found to be necessary and sufficient for phenol reception, though the kinase region must be present for further propagation of the signal. In addition, complete VirA signal recognition has been found to work

in conjunction with the periplasmic protein ChvE, which functions through and interaction with sugar followed by an interaction and enhancing of VirA signaling.

Recently we have characterized a region located between the Periplasmic and Linker domains called the Signal Integration Node (SIN) that has been found to alter phenol recognition and sensitivity (Fang et al., 2015; Swackhammer et al., 2022). Truncations of the SIN have been found to completely alter phenol recognition from the typical phenol acetosyringone (AS) to recognition of dimethoxyphenol (DMP). The tyrosine residue at the 293 locus in the SIN has been shown to be particularly influential in altering response, particularly when mutated to phenylalanine. VirA^{wt} typically functions as a Boolean AND gate, requiring both phenol and sugar recognition to elicit a response; however, with this Y293F mutation, VirA is able to function as an OR gate and only needs one of the signal types to be available to elicit functionality, and the OR gate is also associated with a higher overall VirA response (Fang et al., 2015).

The Linker domain has been modeled to be a GAF domain (cGMP-specific phosphodiesterases, adenylyl cyclases, and FhlA), which are characterized by their ability to bind small molecules. Our current model is that there exists direct binding between the Linker domain and phenols; however, this prediction has not previously been shown experimentally. There also exists a hypothesis that an additional protein or proteins are involved in the process of phenol binding. This hypothesis results from the discovery of phenol-binding surface proteins and experiments suggesting the ChvE-sugar interaction with the Periplasmic domain induces conformational changes in VirA to allow a xenonostic phenol binding protein to mediate signal reception (Dyé

& Delmotte, 1997; Joubert et al., 2002; Campbell et al., 2000). These initial findings, however, seem unlikely given our model predictions.

The aims of my thesis work are to investigate the structure of the VirA Linker domain and test the hypothesis that there is a direct VirA interaction with phenol. Additionally, we are investigating the altered stability and binding capabilities of mutations within the SIN in addition to loci that models have shown to be potentially influential for phenol binding. Through this experimental analysis, we aim to further understand the function and binding abilities of VirA in initiating pathogenesis.

Materials and Methods

B-Galactosidase Assay

A. tumefaciens strain A136, wildtype A348 cells without the Ti plasmid but containing the plasmid pRG109, was transformed through heat shock protocols with plasmids containing VirA^{wt}, VirA^{Y293F}, or VirA^{Y293W} (Table 1). Strains were inoculated into 4 mL LB liquid and incubated overnight at 28°C with shaking. Cultures were back-diluted to an OD₆₀₀ of 0.1 in 2 mL of Induction Media (AB Medium pH5.5, 0.04X AB Buffer, 1X AB Salts). Inducers were added as appropriate (phenols dissolved in DMSO), and cultures were incubated at 28°C with shaking for 16 hours. After incubation, 200 µL induction culture and 800 µL Z-buffer (0.06 M Na₂HPO₄ • 7H₂O, 0.04 M NaH₂PO₄ • H₂O, 0.01 M KCl, 0.001 M MgSO₄ • 7H₂O) were combined. To each tube, 40 µL 0.05% SDS and 40 µL chloroform was added, and tubes were mixed by inverting. Tubes were incubated at room temperature for 10 mins before 200 µL o-NPG (4 mg/mL) was added to each tube. Tubes were allowed to incubate at room temperature for a

sufficient amount of time to observe color change. To terminate the reaction, 200 μL 2.5 M Na_2CO_3 was added to each tube to terminate the reaction. Tubes were centrifuged at 13500 rpm for 3 mins to pellet cell debris, and A_{420} of the supernatant was measured. Measurements were taken in triplicate. To calculate Miller Units of Activity, the following equation was used:

$$\text{Miller Units} = (A_{420} \cdot 10^3 \cdot 7.5) / (X \text{ min} \cdot A_{600})$$

Bacterial Transformation

Rosetta (DE3) pLysS competent cells were used for all assays involving protein. Expression plasmids containing *virA* were either engineered through SLIM mutagenesis, gel purification, and ligation or ordered from GenScript. Once created and miniprepmed using Qiagen kits, 2 μL of the plasmid containing the VirA sequence and 20 μL of Rosetta cells were combined and put on ice for 5 minutes. The mixture was then held in a 42°C water bath for 30 seconds before being put back on ice for 2 minutes. 250 μL Super Optimal broth with Catabolite repression (SOC outgrowth medium) was added, and they were incubated at 37°C in a shaking incubator for 1 hour. The samples were then plated on LB with 0.1 mg/mL of carbenicillin, 0.025 mg/mL chloramphenicol and left overnight in 37°C.

Protein Production

The Rosetta cells that were previously transformed with the VirA plasmid were inoculated in 40 mL LB with 0.1 mg/mL of carbenicillin, 0.025 mg/mL chloramphenicol, and 400 μL of 50% glucose in dH_2O . Cells were grown at 37°C overnight until an OD_{600} of approximately 1.0 was reached. At which point the cells were added to 360 mL SB broth with salts to be shaken at 37°C for 1 hour before inducing protein over-expression with the addition of 0.3 mM isopropyl-1-thio-

D-galactopyranoside (IPTG). The cells were then allowed to grow overnight at 20°C. Samples were then centrifuged and stored at -80°C.

Protein Purification

The frozen pellets were removed from -80°C and allowed to thaw before being resuspended in 12 mL of a lysis buffer containing 10 mM imidazole, 300 mM NaCl and 50 mM NaH₂PO₄•H₂O pH 8.0 in addition to 50 µL AEBSF and a protease inhibitor pill. The cells were lysed through sonication. The protein was purified through TALON immobilized metal affinity chromatography (IMAC) method with 200 mM and 450 mM elution steps.

The protein was then transferred to a 5 mM phosphate buffer using Cytiva PD-10 desalination columns. VirA was then concentrated using Amicon ultra-15 centrifugal filter units with a 10 kDa cutoff to approximately 500 µL.

SDS Page

Protein samples that were collected during the purification process were combined with 4X Laemmli buffer. 15 µL of each sample was added to the wells of a 12% SDS acrylamide gel and ran at 23 mA per gel. Gels were then stained with GelCode Blue Stain reagent.

Fluorescence-Based Thermal Shift (FTS) Assay

Small molecule screening was conducted using the purified VirA with the addition of DMSO, 0.01 µM, 0.1 µM, or 1.0 µM AS dissolved in DMSO. 2.5 µL 50X SYPRO Orange Dye, and 12.5 µL buffer were added to achieve a final volume of 25 µL in each PCR tube. 0.1 µM AS in buffer

was also measured and these values were subtracted from the output of the other samples. The CFX96 Real-Time PCR Detection System was used to collect melt curve data. Samples were run from 10°C to 95°C in increments of 0.5°C per every 10 seconds. Measurements were performed in duplicate.

Circular Dichroism (CD)

CD measurements were taken with a Jasco spectropolarimeter using the final purified VirA protein. Measurements were taken in a range of 200-250 nm. The spectrum of the blank buffer was collected and subtracted from the protein measurements. Data were collected for both VirA^{wt} and VirA^{Y293F}.

Table 1. Strains and Plasmids used in this study

Strains/plasmids	Relevant characteristics	Reference
<i>E. coli</i> strains		
DH5- $\alpha\beta$	<i>recA1, endA1, lacZΔM15</i>	Invitrogen, (Taylor et al., 1993)
Rosetta(DE3) pLysS	<i>dcm, ompT, hsdS(r B - m B -), gal</i>	Millipore
<i>A. tumefaciens</i> strains		
A136	Strain C58 cured of pTi plasmid	(Watson et al., 1975)
Plasmids		
pRG109	<i>P_{N25}-His6-virG, P_{virB}-lacZ</i> in pMON596, IncP, Spec ^r	(Rong Gao & Lynn, 2005)
pJZ6	IncW/Cole expression vector with <i>P_{N25}</i> , Ap ^r	(Lin et al., 2014)
pDP106	<i>virA</i> in pJZ6, Ap ^r	(Swackhammer et al., 2022)
pDP118	<i>virA(Y293F)</i> in pJZ6, Ap ^r	(Swackhammer et al., 2022)

pDP122	<i>virA</i> (Y293W) in pJZ6, Ap ^r	(Swackhammer et al., 2022)
pDP131	His6 tagged <i>VirA</i> (280-471) in pET15b	This study
pDP134	His6 tagged <i>VirA</i> (280-471, Y293F) in pET15b	This study

Results

VirA Structure Modeling Predictions

Structural models for proteins that do not have experimentally solved structures have become a common mechanism for initial investigations into protein structure and developing predictions that can be tested through mutational analysis. The DeepMind AI program AlphaFold has generated many of these models, including for the protein VirA from a variety of *A. tumefaciens* substrains (Jumper et al., 2021; Varadi et al., 2021). The AlphaFold prediction used here utilizes the VirA sequence from strain A348 that has been previously described (UniProt P07167) (Fang et al., 2015; R Gao & Lynn, 2007; Lin et al., 2014), and we have further depicted VirA spanning the bacterial membrane (Fig. 1A). The AlphaFold model predicts VirA to have an α -helix that composes the second transmembrane region (depicted here as α 1 and α 4). The combination of the AlphaFold model and the VirA construction that has been previously described (Fig. 1B) can further the understanding of VirA functionality. This AlphaFold model predicts α 1 to contain 70 amino acids (aa233-302), which is similar to previous predictions (Nair et al., 2011), but to extend its impact, this model is the first to predict that the periplasmic region is connected to the Linker domain.

This AlphaFold model of the Linker domain is also able to provide information on potential AS binding sites. Through the use of the GOLD docking program, we were able to identify four

binding cavities located in very close proximity to the amino acids W355, Q427, R444, and R454 (Fig. 1C). This same GOLD docking program also identified W355 as a potential AS binding site when using a model generated by Phyre2 (Lin et al., 2014). Further investigation will be needed to confirm model predictions about these loci. These structural predictions allow further insight into the protein functionality in *A. tumefaciens*.

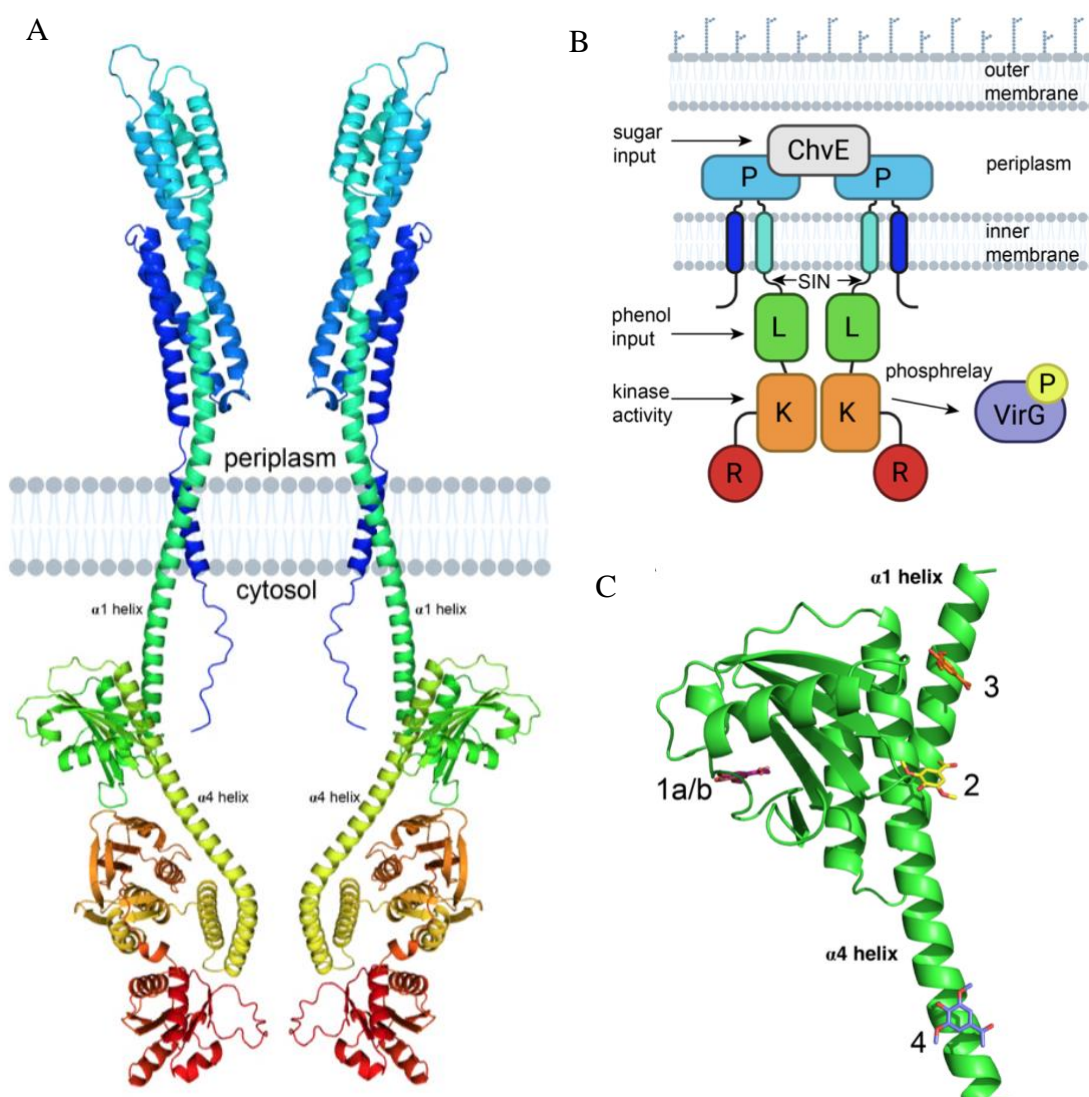


Figure 1. Modeling VirA using AlphaFold. (A) Prediction of VirA (UniProt P07167) structure using AlphaFold (Jumper et al., 2021; Varadi et al., 2021). Pymol-generated model is from the N-terminus (blue) to the C-terminus (red) and shown as a dimer with two membrane-spanning regions per VirA monomer, consistent with previous VirA studies. (B) Schematic model of VirA. (C) The modeling program GOLD was used to predict where the phenol AS could bind the Linker region. Interactions with binding pockets near W355 (1), Q427 (2), R444 (3), and R454 (4) are shown (Modified from Swackhammer et al., 2022).

Y293 Mutations Affect Signal Recognition

The 293 locus in VirA has been shown to be particularly influential in the activity of VirA, affecting the logic gating of the protein when mutated to phenylalanine. VirA^{wt} typically needs both phenol and sugar to be present to elicit a response, but VirA^{Y293F} can function as an OR gate with either one of the signal types to be present (Fang et al., 2015). We furthered this investigation by looking at the effect of a mutation in this locus to a different aromatic amino acid, tryptophan. We found that VirA^{Y293W} follows a very similar response to VirA^{Y293F} when using both AS and DMP as the phenols (Fig. 2). VirA^{wt} has little to no response to any conditions other than both phenol and glucose exposure, while both VirA^{Y293F} and VirA^{Y293W} additionally display activity for only having either phenol or sugar.

These single amino acid substitutions in the 293 locus have a dramatic effect on VirA signal recognition. This severe alteration in activity shows that the 293 amino acid must have some meaningful effect on the structure and binding capabilities of VirA. Further investigation into these Y293 mutations will provide important information about VirA functionality.

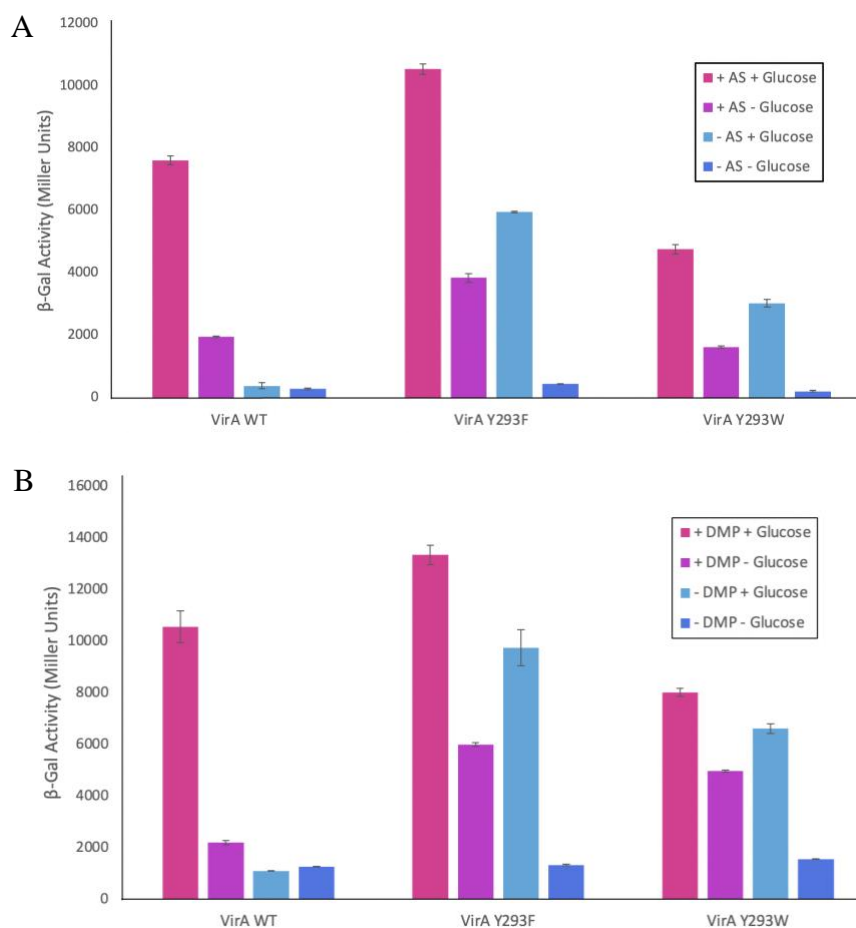


Figure 2. Mutations to the 293 locus affect VirA activity. A. *tumefaciens* strain A136 was transformed with a plasmid containing VirA^{wt}, VirA^{Y293F}, and VirA^{Y293W}. Strains were induced with or without 1% glucose in addition 300 μ M of either the phenol (A) acetosyringone (AS) or (B) dimethoxyphenol (DMP). The β -galactosidase activity was then determined. Bar height represents the mean activity and error bars depict standard error (n=3).

VirA Purification Results

To conduct any experimentation, VirA must first be produced and purified. We completed this through induction in *E. coli* Rosetta cells, followed by lysing the cells, binding the protein to Talon beads, washing away non-specific proteins, and eluting the protein. We do this process to isolate the protein from all other proteins contained in these cells. Through several attempts at optimizing this procedure, we were able to get significant amounts of soluble protein, which are shown for both VirA^{wt} and VirA^{Y293F} (Fig. 3A, B). Both mutants are purified in similar amounts

through a similar procedure, with most of the undesired proteins contained in the flowthrough and initial 5 mM imidazole steps. The VirA protein was most strongly collected with the 200 mM elution rather than 450 mM, allowing us to use the first elution for further experimentation.

Although necessary for observation in various spectroscopic techniques, exchanging buffers appears to have decreased the amount of protein in the sample as can be seen through the buffer exchange and concentrate lanes on both gels. The VirA^{Y293F} has a darker band in the final concentration step, which indicates that there is more protein present in this sample relative to VirA^{wt}. This difference in protein amount could be an indication that the VirA^{Y293F} mutant is more stable throughout this purification process; however, exact quantification will be needed to be performed to confirm if there is indeed a significant difference in the amounts of collected protein. Quantification will also need to be performed for the future experimentation to ensure equal concentrations of protein are being used.

In the elution steps, there are two visible bands at approximately 20 kDa and 40 kDa. The VirA Linker domain that is being used in these experiments would be represented as the band at 20 kDa, so the 40 kDa band could potentially represent a stable VirA dimer. This would be a logical prediction because VirA is believed to function as a dimer; however, using a native gel followed by western blot analysis would be needed to confirm this prediction.

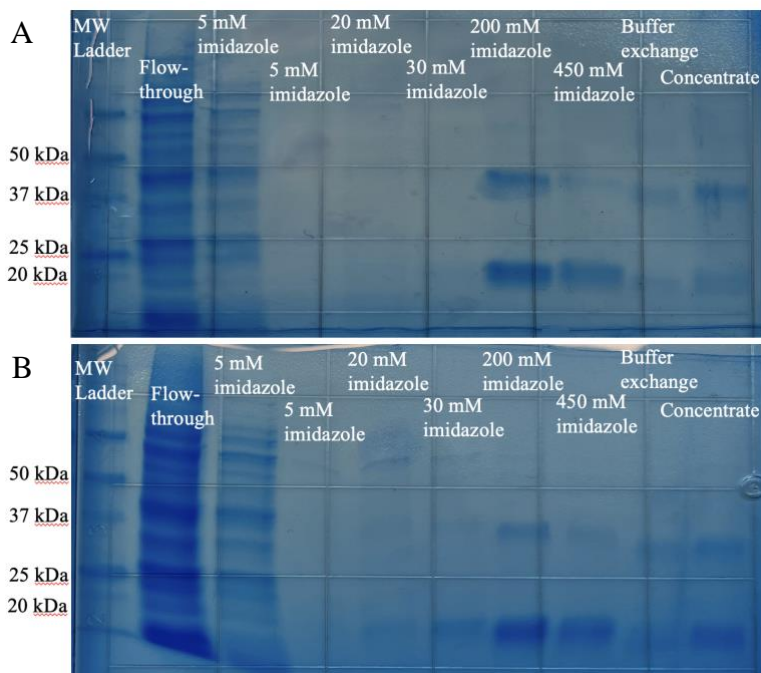


Figure 3. Visualization of purification results of VirA. VirA was produced and purified from Rosetta (DE3) pLysS competent cells. The purified protein then went through a buffer exchange and concentration process. The collected samples from each step of that process were used in SDS PAGE analysis, which was visualized using GelCode Blue Stain reagent. The images show (A) VirA^{wt} and (B) VirA^{Y293F}.

Secondary Structure is Mainly α -helices

Circular dichroism analysis was conducted on both VirA^{wt} and VirA^{Y293F} to obtain information on the secondary structure of the protein. The changes in the mdeg with respect to the wavelength of light depict information on the secondary structure. The data collected from this analysis for VirA^{wt} appear to depict a curve that is indicative of a structure that is mainly comprised of α -helices (Fig. 4); however, it is still somewhat uncertain. The curve does seem to be showing two minima, but it is lacking a high initial peak and steep drop. This smaller magnitude of the curve is notable when comparing the data from VirA^{wt} and VirA^{Y293F}, with VirA^{Y293F} having a higher magnitude. This difference is most likely due to different amounts of protein in the samples used for this analysis. The concentrated elutions were used for this

analysis, and the VirA^{wt} and $\text{VirA}^{\text{Y293F}}$ collections appeared to have different protein concentrations, with $\text{VirA}^{\text{Y293F}}$ having more (Fig. 3).

The curve for $\text{VirA}^{\text{Y293F}}$ appears to be a combination of both α - and β -helices, as shown by its initial high peak followed by a strong drop, indicating prominent α -helices, yet with a single minimum point, which is indicative of β -helices (Fig. 4). Conducting additional experiments with equal concentrations of both proteins would provide more accurate data on their respective structures and any similarities or differences across mutants.

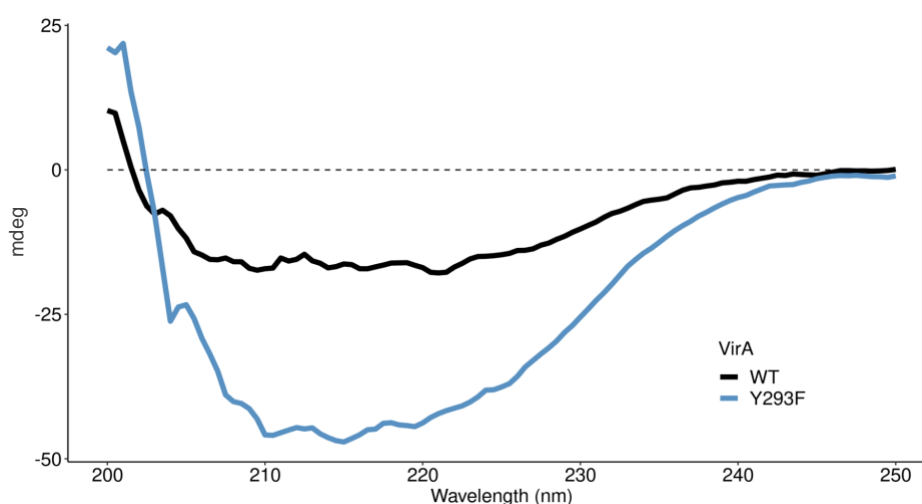


Figure 4. Circular dichroism of VirA indicates mainly α -helix structure. CD spectra of purified VirA^{wt} and $\text{VirA}^{\text{Y293F}}$ were taken at room temperature. Results shown have been baseline corrected with the subtraction of the blank buffer.

VirA^{wt} Directly Interacts with Phenols

Preliminary fluorescence-based thermal shift assays were used to measure VirA stability. These assays can depict changes in stability resulting from ligand binding or mutations (Fig. 5B). We conducted these assays using VirA^{wt} with increasing concentrations of the phenol AS, which has been shown to elicit activity from VirA . The results of this assay show a large difference in the

stability of VirA^{wt} without phenol compared to the protein combined with all concentrations of AS, which all had almost identical curves (Fig. 5A). VirA without any exposure to AS denatured at a lower temperature, suggesting lower stability, which indicates that VirA^{wt} does have direct interactions with AS.

The minimum relative fluorescence measured in these experiments only reaches approximately 70% (Fig. 5A), which signifies denaturation of the protein has begun to occur prior to the start of this assay. Future modifications will need to be done to increase the stability of the protein to conduct these measurements more accurately.

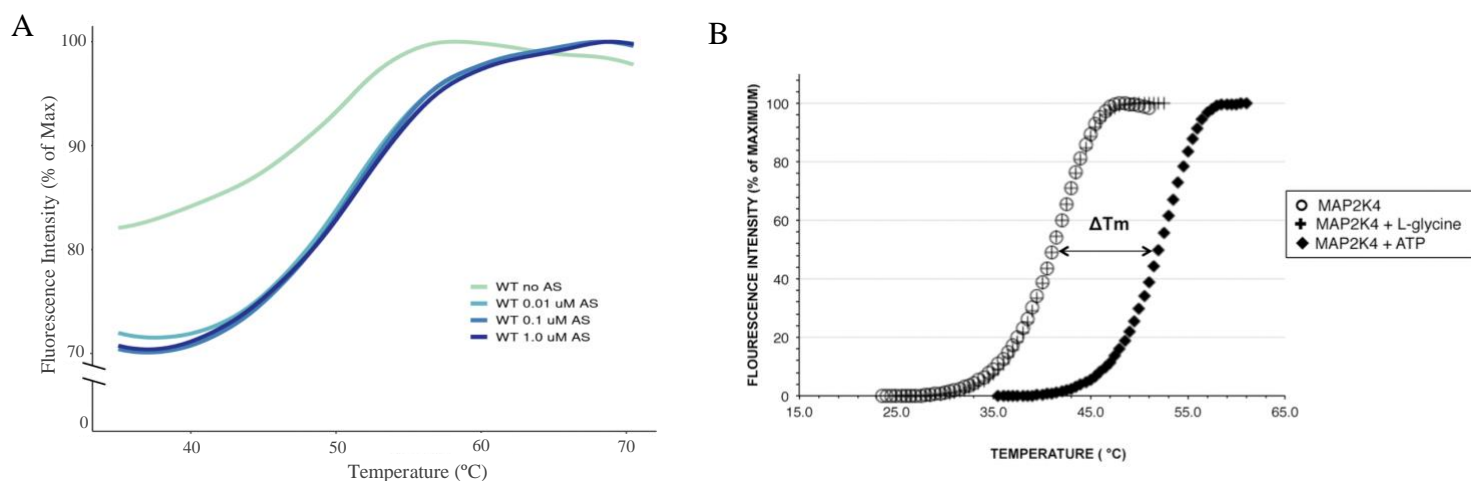


Figure 5. VirA^{wt} stability changes when exposed to AS. (A) Purified VirA^{wt} was combined with SYPRO Orange Dye and increasing concentrations of AS before being exposed to increasing temperatures where fluorescence was measured. Data is plotted as a percentage of the maximum (n=2). (B) Sample thermal shift data showing the change in melting temperature of protein MAP2K4 when exposed to its ligand ATP (Modified from Krishna et al., 2013).

Discussion

The structure and exact function of the VirA Linker domain has long been hypothesized, and my thesis work has begun to fill these gaps of knowledge. Through AlphaFold model predictions

and these initial experimental findings, we can obtain a further understanding of how VirA functions in the pathogenic mechanism of *A. tumefaciens*.

The protein collection process used here had flaws, including prominent loss of protein in the desalination process and denaturation prior to any experimentation (Fig. 2, 4). This inadequate approach leads to experimentation with samples that yield results that become hard to interpret. For further investigation, it may be necessary to create new constructs in order to optimize this process and increase protein stability. Western blot analysis will also need to be conducted to confirm results of the SDS PAGE analysis.

The circular dichroism analyses that were conducted reveal a secondary structure of VirA^{wt} that is indicative of majority α -helices (Fig. 3). This result aligns markedly with the AlphaFold model in addition to previous predictions (Nair et al., 2011). This is the first experimental measure of the Linker domain's secondary structure, which affirms previously stated hypotheses and allows for further investigation into the VirA structure. The VirA^{Y293F} results suggest a combination of both α - and β -helices, which suggests that the Y293F mutation could have impacts on the secondary structure of VirA. Future investigations using identical amounts of protein for the analyses will be necessary to confirm these findings and more accurately understand the differences caused by this mutation. Further research should be done with other amino acid mutations in the Linker domain to see what effects they may have on structure and function. Investigating any secondary structure changes in VirA in the presence of its ligand would depict direct phenol binding and could provide insight into how this interaction occurs.

The thermal shift assays conducted here are the first experimental depiction of direct interaction between the Linker domain and phenol. This confirms the hypothesis of direct phenol binding that was initially supported by models predicting the structure to be a GAF domain. Future investigations into the effect of mutations on stability and phenol binding will also provide significant insight into the function of VirA and where phenol binding may occur. The Y293F mutation has altered sensitivity to phenol, eliciting an increased response to both the phenols AS and DMP in addition to a response from sugar alone (Swackhammer et al., 2022). Additional thermal shift analysis into this mutant in this variety of conditions in addition to other VirA mutants will further understandings surrounding VirA functionality.

Because *A. tumefaciens* causes such significant damage to plants, any further understanding of how this pathogenic mechanism occurs can be greatly beneficial towards minimizing this harm. VirA is the protein that is responsible for the initial step in this pathogenesis, so investigation into this protein's ability to recognize signals will likely lend significant benefits towards preventative measures.

References

- Campbell A. M., Tok J. B., Zhang J., Wang Y., Stein M., Lynn D. G., Binns A. N. (2000) Xenognostic sensing in virulence: Is there a phenol receptor in *Agrobacterium tumefaciens*? *Chem. Biol.* 7: 65-76.
- Clemens C. Heikaus, Jayvardhan Pandit, Rachel E. Klevit (2009). Cyclic Nucleotide Binding GAF Domains from Phosphodiesterases: Structural and Mechanistic Insights. *Structure*. 17(12): 1551-1557. <https://doi.org/10.1016/j.str.2009.07.019>.
- Dyé F. & Delmotte F. M. (1997). Purification of a protein from *Agrobacterium tumefaciens* strain A348 that binds phenolic compounds. *Biochem. J.* 321, 319-324

- Fang, F., Lin, Y.-H., Pierce, B. D., Lynn, D. G. (2015). A Rhizobium radiobacter Histidine Kinase Can Employ Both Boolean AND and OR Logic Gates to Initiate Pathogenesis. *Chembiochem. Eur. J. Chem. Biol.* 16, 2183–2190. doi: 10.1002/cbic.201500334
- Gao, R & Lynn, D. G. (2007). Integration of Rotation and Piston Motions in Coiled-Coil Signal Transduction. *Journal of Bacteriology*, 189(16), 6048–6056. <https://doi.org/10.1128/jb.00459-07>
- Gao, Rong & Lynn, D. G. (2005). Environmental pH Sensing: Resolving the VirA/VirG Two-Component System Inputs for Agrobacterium Pathogenesis. *Journal of Bacteriology*, 187(6), 2182–2189. <https://doi.org/10.1128/jb.187.6.2182-2189.2005>
- Graves, A. E., Goldman, S. L., Banks, S. W., Graves, A. C. (1988). Scanning electron microscope studies of Agrobacterium tumefaciens attachment to Zea mays, Gladiolus sp., and Triticum aestivum. *J. Bacteriol.* 170, 2395–2400. doi: 10.1128/jb.170.5.2395-2400.1988
- Joubert P., Beaupère D., Lelièvre P., Wadouachi A., Sangwan R. S., Sangwan-Norreel B. S. (2002). Effects of phenolic compounds on Agrobacterium vir genes and gene transfer induction – a plausible molecular mechanism of phenol binding protein activation. *Plant Sci. J.* 162 733-743.
- Jumper, J., Evans, R., Pritzel, A., Green, T., Figurnov, M., Ronneberger, O., Tunyasuvunakool, K., Bates, R., Žídek, A., Potapenko, A., Bridgland, A., Meyer, C., Kohl, S. A. A., Ballard, A. J., Cowie, A., Romera-Paredes, B., Nikolov, S., Jain, R., Adler, J., ... Hassabis, D. (2021). Highly accurate protein structure prediction with AlphaFold. *Nature*, 596(7873), 583–589. <https://doi.org/10.1038/s41586-021-03819-2>
- Krishna, S. N. et al. A fluorescence-based thermal shift assay identifies inhibitors of mitogen activated protein kinase kinase 4. *Plos One* 8, e81504 (2013).
- Lin, Y.-H., Pierce, B. D., Fang, F., Wise, A., Binns, A. N. & Lynn, D. G. (2014). Role of the VirA histidine autokinase of Agrobacterium tumefaciens in the initial steps of pathogenesis. *Frontiers in Plant Science*, 5, 195. <https://doi.org/10.3389/fpls.2014.00195>
- Liu, S., Lin, Y.-H., Murphy, A., Anderson, J., Walker, N., Lynn, D. G., Binns, A. N., Pierce, B. D. (2020). Mapping reaction-diffusion networks at the plant wound site with pathogens. *Front. Plant. Sci.* 51(4): 707-16. <https://doi.org/10.3389/fpls.2020.01074>
- McCullen C.A., Binns A.N. (2006). Agrobacterium tumefaciens and plant cell interactions and activities required for interkingdom macromolecular transfer. *Annu Rev Cell Dev Biol.* 22:101-27. doi: 10.1146/annurev.cellbio.22.011105.102022. PMID: 16709150.
- Nair, G. R., Lai, X., Wise, A. A., Rhee, B. W., Jacobs, M. & Binns, A. N. (2011). The Integrity of the Periplasmic Domain of the VirA Sensor Kinase Is Critical for Optimal Coordination of the Virulence Signal Response in Agrobacterium tumefaciens ‡. *Journal of Bacteriology*, 193(6), 1436–1448. <https://doi.org/10.1128/jb.01227-10>

- Swackhammer, A., Provencher, E., Donkor, A. K., Garofalo, J., Dowling, S., Garchitorena, K., Phyto, A., Ramírez Veliz, N., Karen, M., Kwon, A., Diep, R., Norris, M., Safo, M. K., & Pierce, B. D. (2022). Mechanistic Analysis of the VirA Sensor Kinase in *Agrobacterium tumefaciens* Using Structural Models. *Frontiers in microbiology*, *13*, 898785. <https://doi.org/10.3389/fmicb.2022.898785>
- Varadi, M., Anyango, S., Deshpande, M., Nair, S., Natassia, C., Yordanova, G., Yuan, D., Stroe, O., Wood, G., Laydon, A., Židek, A., Green, T., Tunyasuvunakool, K., Petersen, S., Jumper, J., Clancy, E., Green, R., Vora, A., Lutfi, M., ... Velankar, S. (2021). AlphaFold Protein Structure Database: massively expanding the structural coverage of protein-sequence space with high-accuracy models. *Nucleic Acids Research*, *50*(D1), D439–D444. <https://doi.org/10.1093/nar/gkab1061>
- Watson, B., Currier, T. C., Gordon, M. P., Chilton, M. D. & Nester, E. W. (1975). Plasmid required for virulence of *Agrobacterium tumefaciens*. *Journal of Bacteriology*, *123*(1), 255–264. <https://doi.org/10.1128/jb.123.1.255-264.1975>